Title	Experimental mechanical testing of Poly (l-Lactide) (PLLA) to facilitate pre-degradation characteristics for application in cardiovascular stenting
Author(s)	Bobel, Anna C.; Lohfeld, Stefan; Shirazi, Reyhaneh Neghabat; McHugh, Peter E.
Publication Date	2016-07-19
Publication Information	Bobel, Anna C., Lohfeld, Stefan, Shirazi, Reyhaneh Neghabat, & McHugh, Peter E. (2016). Experimental mechanical testing of Poly (l-Lactide) (PLLA) to facilitate pre-degradation characteristics for application in cardiovascular stenting. Polymer Testing, 54, 150-158. doi: http://dx.doi.org/10.1016/j.polymertesting.2016.07.011
Publisher	Elsevier
Link to publisher's version	http://dx.doi.org/10.1016/j.polymertesting.2016.07.011
Item record	http://hdl.handle.net/10379/6325
DOI	http://dx.doi.org/10.1016/j.polymertesting.2016.07.011

Experimental mechanical testing of Poly (L-Lactide) (PLLA) to facilitate pre-degradation characteristics for application in cardiovascular stenting

Anna C. Bobel, Stefan Lohfeld, Reyhaneh Neghabat Shirazi, Peter E. McHugh

Biomechanics Research Centre (BMEC), Biomedical Engineering, College of Engineering and Informatics, NUI Galway, Ireland

a.bobel1@nuigalway.ie

stefan.lohfeld@nuigalway.ie

reyhaneh.shirazi@nuigalway.ie

peter.mchugh@nuigalway.ie

Abstract

Next-generation stents made from Biodegradable Polymers (BPs) aim to address the long-term risks (i.e. late restenosis and in-stent thrombosis) associated with both Bare Metal Stents and Drug Eluting Stents, whilst aiming to reduce the healthcare costs associated with secondary care. However, the true potential of BPs for cardiovascular load bearing applications does not appear to be fully realised. While the literature provides data on stiffness and strength of BPs, it is lacking pre-degradation experimental data on the recovery behaviour and temperature and strain rate dependency. In this paper, an experimental study is undertaken to address this knowledge gap using Poly (L-Lactide) (PLLA) samples, subjected to tensile testing. Stress-strain characteristics, recovery, relaxation and creep data at body temperature are reported and considered in the context of real-life stent deployment. The experimental data herein reveal a strong temperature and strain rate dependency, whilst demonstrating associated plasticity within the material. The work provides a physical evaluation of PLLA's pre-degradation behaviour, establishing key data points to allow the assessment of PLLA as a viable material in the wider context of stent deployment and load carrying capacity.

1. Introduction

Biodegradable Polymers (BPs), in particular Poly (L-Lactide) (PLLA), have emerged as a favourable choice for use in orthopaedics and interventional cardiology medical devices [1, 2]. On a small clinical scale, PLLA's reliability as a viable stent material, chosen to overcome complications experienced with conventional metal stents (e.g. restenosis and thrombosis), has been demonstrated [3]. More specifically, the potential attractiveness of PLLA is confirmed by the commercialisation of the first fully biodegradable polymer stent "Absorb" (Abbott Vascular, USA), whilst there are a number of other competitive products in the pipeline [4-6]. To date, the benefits of non-permanent stents are increasingly recognised and widely reported in numerous publications [7-9]. The main advantages include (i) reduced in-stent restenosis, (ii) minimisation of late thrombosis risk, and (iii) reduction in restriction that the flexibility of a polymer affords for artery expansion and contraction, minimising physical changes in everyday function [10].

Given these recent advancements coupled with the capabilities of simulation software, it could be assumed that the mechanical performance of PLLA in the context of the stent application is understood and widely reported. However, this is far from being the case due to the confidential nature of the medical device industry, further complicated by the small volume and short-term existence of these products on the market. As a consequence, there is still a substantial lack of knowledge regarding the loading capacities, plastic deformation, recovery and general behaviour of PLLA, as reported by Bobel et al. [11]. Such mechanical uncertainty poses un-predictable risks as the loading characteristics are vital for safe and effective clinical performance of cardiovascular stents. A lack of confidence in reliable performance has had a negative impact on BPs becoming a disruptive technology as an alternative to BMS and DES [7]. The capability of computational modelling is also compromised; without this accurate

experimental data, simulative design optimisation studies cannot reach their full potential (i.e. reduce costs, predict long-term performance, inform decisions based on reliability, etc.).

A number of clinical trials that may help our understanding and generate further confidence in bioabsorable stents are either underway or in the planning phase. Abbott Vascular recently announced a clinical trial involving 3,000 patients for their next generation stent, the Absorb IV [12]. The Amaranth FORTITUDE stent successfully completed clinical trials and further studies for the second-generation FORTITUDE stent are planned [13]. Elixir DESolve and REVA Fantom completed first-in-man trials and additional clinical trials involving >100 patients [14, 15]. In contrast, there are no clinical performance progress reports published recently on the Arterial Remodelling Technologies (ART) stent or the first fully bioabsorable stent, the Igaki-Tamai stent. Interestingly, a recent study by Varcoe et al. [16] indicates a high Target Lesion Revascularisation (TLR) rate in the long term study of the Igaki-Tamai stent, strongly suggesting that this particular stent system is not suitable for clinical consideration.

The existence and increasing availability of degradation performance data for PLLA is apparent [17], unfortunately, this is not the case for pre-degradation mechanical performance data. For example, PLLA is known to degrade slowly (>24 months), meaning it can provide mechanical stability for >6 months [18, 19]. The limited amount of pre-degradation data is surprising when considering the importance of loading capacity, plastic deformation and recoil at stent deployment. More specifically, the mechanical properties of PLLA, such as elastic modulus, mechanical strength and ductility, are of major interest and importance when the material is subjected to high loads during stent deployment [20]. The mechanical properties are strongly related to the physical properties of the material, e.g. molecular weight, inherent viscosity and crystallinity, as well as melting and glass transition temperatures [21]. The molecular weight of a polymer strongly affects the mechanical behaviour and degradation rate [20]. The inherent viscosity is linked to the molecular weight defined by the Mark–Houwink equation [22], and an increasing molecular weight leads to a rise in inherent viscosity. The deployment instructions for Abbott's Absorb stent suggest a slow and gradual expansion with a balloon pressure increase of 2 atm every 5 seconds to a maximum pressure of 16 atm. This indicates a dependency of the material behaviour on the deployment rate.

There are a limited number of experimental studies evaluating the mechanical performance of pure PLLA. Among the few reports that are available, Grabow et al. focused on the stent application and examined various different mechanical characteristics of fully polymeric PLLA stent deployment (stent recoil and shortening, pressure vs. diameter change and creep at constant pressure) [23]. An earlier study by Grabow et al. investigated mechanical properties of rod and dumbbell samples of pure PLLA and PLLA/TEC [24]. A retardation curve (creep and relaxation behaviour), as well as modulus and tensile strength, with modulus variation as a function of temperature, were presented. A study by Eswaran et al. [25] presented cyclic data of a PLLA single stent ring element. Wong et al. [26] reported strain rate dependency of PLLA at body temperature and stress-strain behaviour at body temperature and glass transition temperature (50°C). In contrast, the change in properties during degradation for PLLA has been more extensively studied, for example [17, 27]; consideration was also given to a variety of

material compositions of PLLA, and how these combinations could enhance performance in comparison to pure PLLA.

Given the lack of full mechanical characterisation data for pure PLLA material pre-degradation, there is an absence of a comprehensive reported evaluation of PLLA in relation to the loading histories that are experienced during real-life stent deployment, and this has hindered the progression of the use of this material. Specific characterisation data such as that related to unloading behaviour, including recoverable elastic strain, viscoelastic strain and permanent plastic deformation, are largely absent in the reported literature. The authors strongly believe that the presentation of such data can facilitate the development of enhanced BP stents by addressing the gap in reported knowledge and the related uncertainty of performance prediction.

In view of the limitations summarised above, this paper presents an experimental characterisation of PLLA material relevant to the stent application in the pre-degradation state. The study focuses on mechanical performance, i.e. stress-strain behaviour, addressing strain rate dependence, relaxation, recovery, temperature dependence and plastic deformation. It is acknowledged that temperature dependent data is vital for accurate stent deployment assessment. Such data can vary between room temperature (pre-implantation) and values exceeding normal body temperature up to 42°C (possible reaction/inflammation to the implant). To this end, the significant role of temperature variation and strain rate dependency is reported.

2. Materials and Methods

2.1 Material

The PLLA polymer used in this study, Purasorb® PL 65, was supplied by Corbian-Purac Biomaterials (Gorinchem, Netherlands) in granular form. This high molecular weight PLLA has an inherent viscosity of 6.5 dL/g and a molecular weight of 481,500 g/mol. The solvent Dichloromethane (DCM) was purchased from Sigma-Aldrich (County Wicklow, Ireland).

2.2 Sample Preparation

Test specimens were prepared by solvent casting. PLLA was dissolved in DCM with a concentration of 0.03g/ml (see Figure 1) at room temperature under constant stirring over a period of 72 hours or until fully dissolved. The solution was then poured into a glass petri dish with a diameter of 10 cm to generate a thin film sheet with a thickness of 200 μm (±30). The dish was covered with a lid until the DCM was fully evaporated, which was subsequently confirmed by a constant weight of the PLLA sheet.
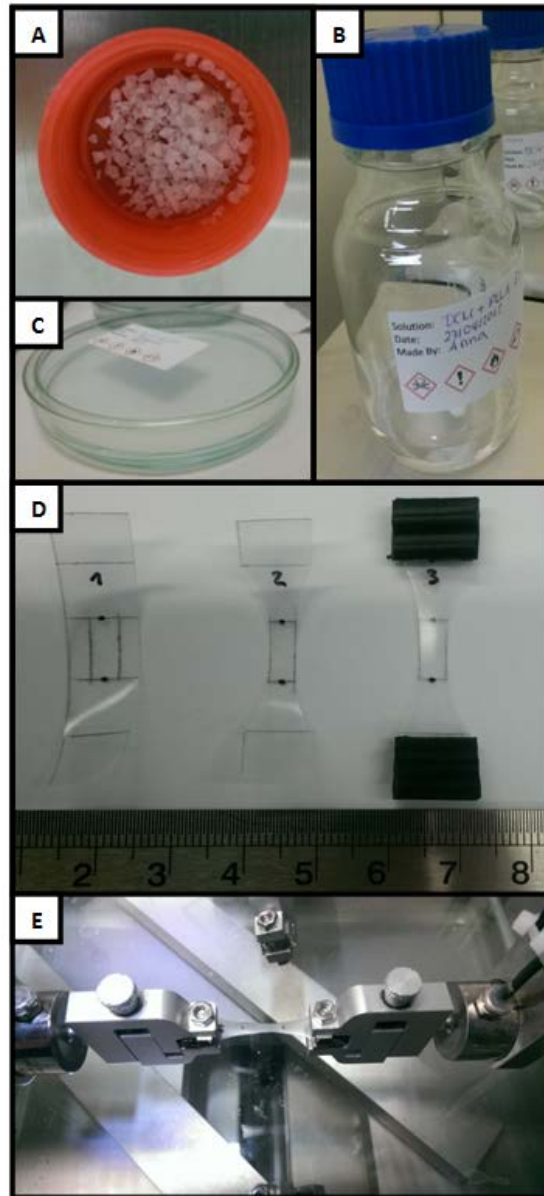
Figure 1 Specimen preparation: A - PLLA granules, B - PLLA-DCM solution, C - Glass dish with PLLA solution, D - PLLA film specimen and rubber grip preparation, E - PLLA specimen in tensile testing machine.

The authors are cognisant of the potential impact that the manufacturing technique can have on the mechanical performance of the material. The solvent casting method was selected as a proven thin film production technique for tensile sample preparation, ensuring the preparation of uniform specimens of a stent application size-scale. The ease of use of this method allows faithful control of thickness throughout the sample. However, it is acknowledged that there is a range of component/device manufacturing processes that could be used in practical application and that these would have an impact on mechanical properties.

Dumbbell shaped specimens were cut from the thin sheet with a gauge length of 10 mm (±0.3) and a width of 4 mm (±0.5) (according to ISO 527-3 and ISO 527-1) for mechanical testing. A

stiff rubber pad was glued on each end of the specimen to help avoid slip during testing. A number of grips were examined prior to the experiments described below. A glued rubber strip was found to prevent slippage with reasonable reliability.

2.3 Testing

<u>Equipment</u>

A Zwick bi-axial tensile testing machine (Zwick, Ulm, Germany) with a 100N load cell, TestXpert software, and a connected video extensometer with VideoXtense software was used, in uni-axial mode, to determine the mechanical performance of the material. Specimens tested at temperatures higher than room temperature (37°C and 42°C) were tested in a water bath with an under-heating mat attached to the tensile testing machine. At all time, samples tested at higher temperature remained in the water bath while being tested. The water temperature was constantly monitored using a digital thermometer placed in the bath. The temperature distribution and heat flow within the specimens was monitored using a Flir One thermal camera (FLIR Systems, Wilsonville, OR, USA).

<u>Testing Methods</u>

122 specimens were tested. For all specimens the elongation in the specimen gauge was measured and recorded using the video extensometer and software package. From this, engineering strain was calculated as the change in gauge length over original gauge length. The force was measured by the load cell and, subsequently, the engineering stress within the material was calculated. Both load and displacement controlled testing was performed. The stress-strain plots presented below consider engineering stress and strain. A representative stress-strain curve including recovery is shown in Figure 2. The strain on unloading can be divided into i) elastic strain that is instantaneously recoverable, ii) viscoelastic strain, which is recoverable over time, and iii) plastic strain which refers to unrecoverable deformation of the material.
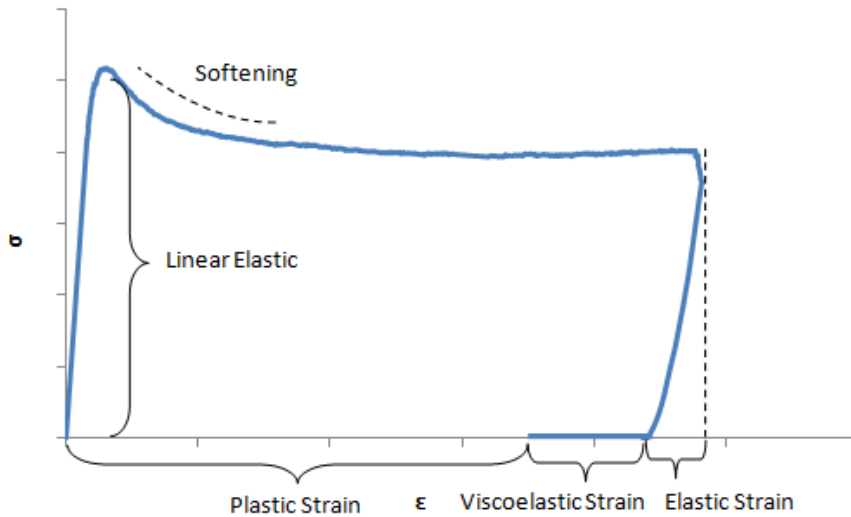
Figure 2 Terminology to describe typical stress-strain behaviour of a PLLA polymer upon loading and unloading.

Uni-axial Tensile Test

Displacement controlled uni-axial tensile tests with load removal were performed with varying maximum crosshead displacement and displacement rates, generating variations in maximum strain and strain rate in the specimen gauge. Test temperature was also varied. Applied crosshead displacement rates were in a range consistent with conditions commonly reported in the literature [28, 29]. These crosshead displacement rates are considered to apply overall 'strain rates' to the specimens. Table 1 shows the displacement rates used in this study and the corresponding applied strain rates, calculated based on the sample size. For each applied displacement history, the actual engineering strain in the sample gauge was determined from the video extensometer measurements of the change in gauge length. In this particular setup, unloading was performed rapidly and the test was stopped immediately on unloading, therefore it does not reflect the full material recovery which is addressed in a different test (Recovery test).

Displacement Rate (mm/min)		Strain Rate (1/s)
1	≜	1.3×10^{-3}
10	≜	1.3×10^{-2}
100	≜	1.3×10^{-1}
2.5	≜	3.25×10^{-2}
5	≜	6.5×10^{-2}

Table 1 Displacement rates and corresponding strain rates for specimen manufactured for this study.

Recovery

The recovery of the material was assessed by stretching the sample to a set crosshead displacement, followed by subsequent force controlled unloading. Over a time span of 5 minutes, the force was set to a target of 0N in order to assess the recovery of the sample.

Relaxation-Creep

Relaxation is defined as a decrease in stress in response to a constant applied strain. Here, a version of such a test was performed, based on a set crosshead displacement, that was applied to the specimens and the stress and gauge strain were observed over a time period of 5 minutes.

Cyclic Loading

Load was applied based on a set displacement. When reached, the specimen was unloaded, followed by re-loading with an increased displacement at every step. This test consists of five repetitions with an applied strain load of 5 - 10 - 15 - 20 - 25%.

Temperature Variation

Room temperature (RT) - specimens were tested at approximately 25°C. Body temperature (BT) - specimens were tested in a water bath with a temperature of 37°C. High temperature (HT) - specimens were tested in a water bath with a temperature of 42°C. Specimens were inserted into the heated water bath and subsequently tested. Initial testing showed a fast heat distribution throughout the thin film specimens. This subsequently implies fast cooling rates when removed from the water bath. However, since the specimens were inside the water bath at all times during the test, the cooling rate is not relevant. The temperature range (25 to 42°C) for the study was selected to be reflective of real-life stent conditions. Material hydrolysis was completely neglected in this study, considering that the short testing time in the range of minutes does not have an impact on short term material performance [30].

Crystallinity

The crystallinity properties of PLLA samples were also examined via Differential Scanning Calorimetry (DSC) to evaluate the crystallinity, since mechanical properties strongly relate to the degree of crystallinity.

3. Results

Mechanical testing of thin PLLA specimens can be very challenging, confirmed by the very limited data reported in literature. In this study, a total of 122 specimens were examined, with 63% of specimens successfully tested. In relation to unsuccessful tests, issues encountered in this study included gripping and slippage due to the material mismatch between sample and testing apparatus. To account for this issue, only the strain measured at the gauge area was utilised. It is acknowledged that the testing machine applies a displacement based on the overall geometry, meaning that an exact specimen strain can sometimes be difficult to replicate

between various specimens. However, these differences are seen as negligible in the overall context of the experiments. Another problematic issue was overshooting during unloading, particularly when tested in a water bath, as the water embodies a resistance to the load cell. Additionally, the water and flowing particles in the water can distort the video extensometer image. All the aforementioned reasons, in part, contributed to a significant amount of failed specimens within the testing process (37% of the specimens produced unusable results-). Finally, to aid clarity of present ation, the following stress-strain plots show typical stress-strain curves for the different conditions, unless otherwise stated.

DSC Testing

The DSC thermogram of the PLLA sample is shown in Figure 3. The melting temperature and the total crystallinity for the PLLA sample were determined to be 173.6 °C and 41.1%, respectively.
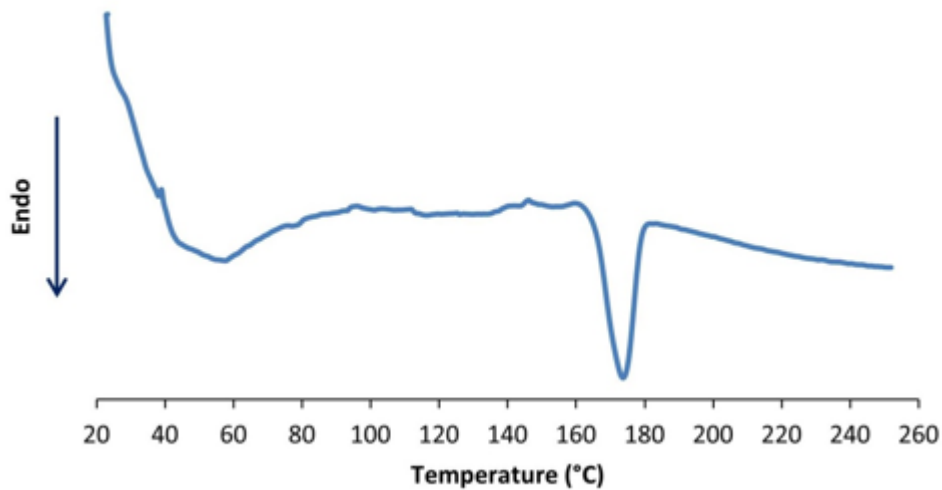

Figure 3 DSC thermogram.

Uni-axial Tensile Test

The load-unload uni-axial tensile test was performed as described above. To get an overview on the mechanical performance of the material, different displacement rates between 1 and 100 mm/min and a relatively large maximum displacement (generating a maximum applied strain of ~150%) were applied in the initial series of tests. It was observed that the material was more likely to fracture if stretched at a higher rate. The test was performed at room temperature (RT), body temperature (BT), and high temperature (HT) (Figure 4). At room temperature and a displacement rate of 100 mm/min, the sample ruptured before unloading, as illustrated in Figure 4(a). The experimental set-up did not allow to reliably apply higher temperatures over an extended period of time, hence the HT experiment was performed with only two higher strain rates (10 and 100 mm/min), as illustrated in Figure 4(c). In general, higher peak stresses were observed with an increase of strain rate, as anticipated (PLLA is known to be a highly rate dependent material). Within the constraints of the temperature range investigated,

temperature was found to have a major effect on the material behaviour. More specifically, at room temperature the material deformed initially in a linear elastic manner before the material experienced peak stresses and softening at higher strains. At higher temperature, the material was generally more compliant and the stress-strain curve more uniform, with a smoother transition between the initial linear elastic response and the non-linear response at larger strain, which was also visible during the tests.
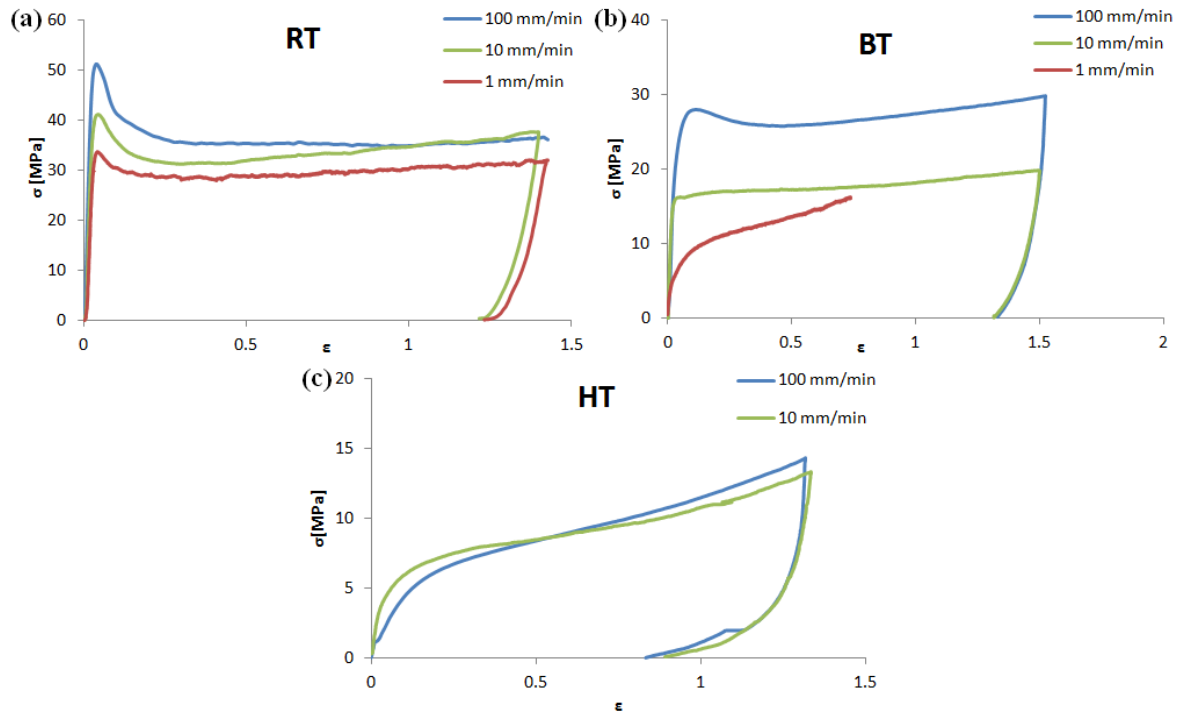

Figure 4 Experimental stress-strain behaviour at different displacement rates: (a) At room temperature (25°C), (b) at body temperature (37°C), and (c) at high temperature (42°C).

Stents typically experience strains of up to approximately 50% during deployment. Furthermore, the recommended deployment rate for the Abbott Absorb stent approximately corresponds to the strain rate occurring at a displacement rate of 2.5 mm/min [31]. Consequently, the experiments were designed around these two values for applied strain and displacement rate, and displacement rates of 1, 2.5 and 5 mm/min up to a maximum strain of 50% were used in the subsequent experiments. Figure 5(a) shows room temperature stress-strain curves for this situation, and displacement rate dependency of the mechanical response is evident.

Focusing on the 2.5 mm/min displacement rate, i.e. Abbott's recommended stent deployment rate, Figure 5(b) clearly shows a high temperature dependency for the material, with the high temperature resulting in a much more compliant response. It was also found that on rapid unloading the material released larger elastic strains at high temperature, indicating increased recoverability at this temperature.

Figure 5(c) presents a typical data spread within repeated tests at room temperature for an overall displacement rate of 2.5 mm/min. As the figure illustrates, reasonable repeatability was generally achieved. However, the data was partly affected by inconsistent room temperature,

which reflects the variation in the material softening step. Also, at the point of unloading, a variation in maximum strains within the gauge region could be observed, whereas the applied strain, as determined by the crosshead displacement, was fixed. This behaviour was characteristic of the tests reported in this work generally; it is more than likely due to a combination of specimen deformation outside the gauge region and the connection between the crosshead grip and the specimen, and it is possibly also influenced by the elasticity of the rubber grips. However, it is important to emphasise that the strain data presented here is the gauge strain only (strain actually measured in the gauge region), and therefore represents the true deformation of the material itself.
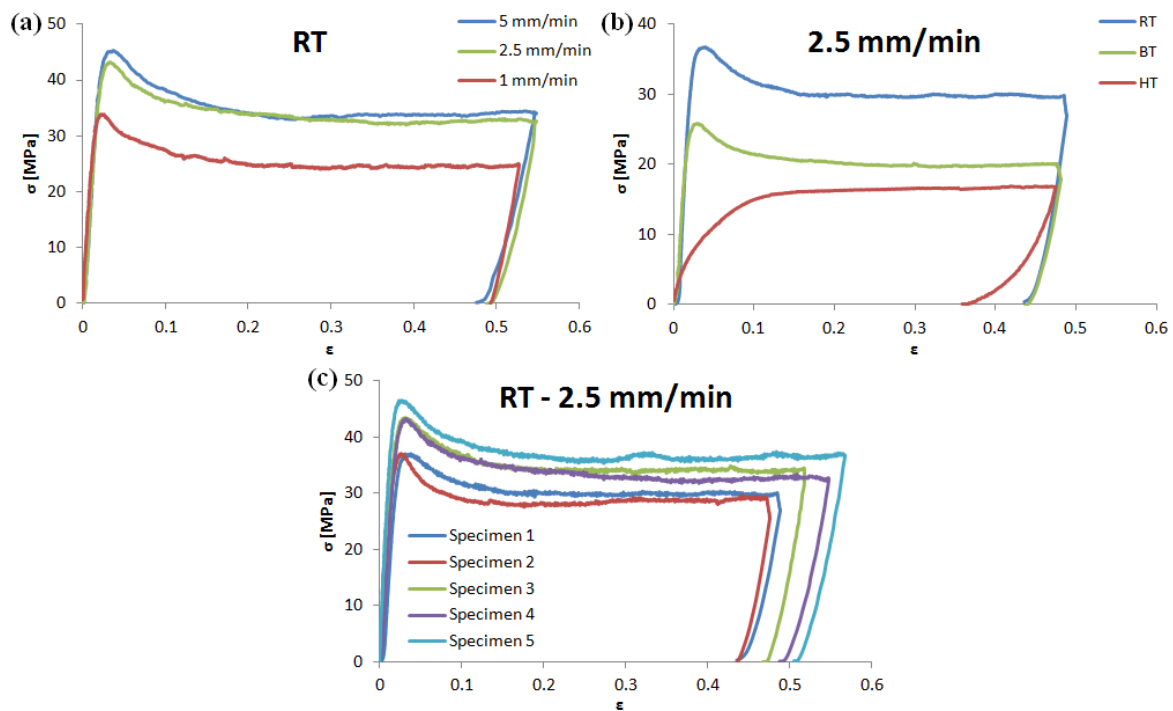

Figure 5 Experimental stress-strain behaviour with max displacement of 50%: (a) At room temperature (25°C) and different displacement rates, (b) at different temperatures and a displacement rate of 2.5 mm/min, and (c) distribution of data over a number

Recovery

Figure 6(a) shows the recovery behaviour of the PLLA samples for the three temperatures considered here. These results provide valuable information on the relative amounts of elastic (instantaneously recoverable), viscoelastic (time dependent recoverable), and plastic (permanent) strain (as defined in Figure 2) in the material during tensile loading. The respective strains are tabulated in Table 2. While the specimens in Figure 6(a) are strained to dissimilar extent (due to the effects discussed above), it can be observed that the overall ability to recover strain increases with temperature. The quantification of elastic strain and viscoelastic strain in Figure 6(a) allows for the calculation of total recoverable strain versus temperature (Figure 6(b)). This data is of major importance for the polymer stent deployment, as it acts as an indicator of recoil. The substantial decrease in permanent plastic strain in the material for a small temperature increase of 5°C between body temperature (37°C) and high temperature

(42°C) is significant (a reported difference of 44.5% in this study), and has important implications for the utilisation of PLLA in the balloon expandable stent application.

	RT	BT	HT
Max ε	0.51 (Total Strain (TS))	0.4 (TS)	0.45 (TS)
Elastic ε	0.06 (12% of TS)	0.06 (15% of TS)	0.25 (55% of TS)
Viscoelastic ε	0.04 (8% of TS)	0.07 (18% of TS)	0.1 (22.5% of TS)
Plastic ε	0.41 (80% of TS)	0.27 (67% of TS)	0.1 (22.5% of TS)

Table 2 Quantitative strain analysis on recovery, for a loading displacement rate of 2.5 mm/min (referring to Figure 6(a)). Strains are also given as percentages of total strain.
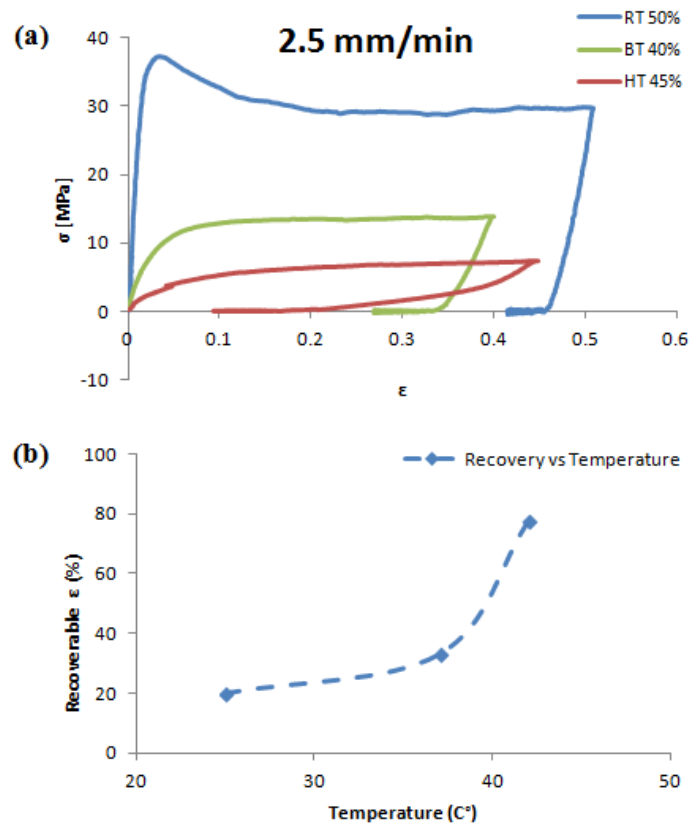

Figure 6 Recovery test: (a) Experimental stress-strain response for the recovery test at different temperatures and maximum gauge strains, with a constant loading displacement rate of 2.5 mm/min, and (b) recoverable strain (as a percentage of total strain) as a function of temperature, over a temperature range of 25 to 42°C.

Relaxation-Creep

Figure 7(a) captures the relaxation behaviour after an initial sample deformation to ~50% gauge strain. Stress relaxation began following maximum crosshead displacement, and the stress

decreased. As a result, it should be noted that the displacement rate given in Figure 7(a) only applies to the loading phase. As can be seen from Figure 7(a), the sample continued to strain in the gauge during the stress relaxation process, given that it was the overall crosshead displacement and not the gauge strain that was fixed, leading effectively to a combined behaviour of relaxation and creep. A full stress relaxation (to zero stress) was not achieved during this test. Figure 7(b) illustrates solely the stress relaxation behaviour vs. time for the three different loading rates at room temperature. Consistent with Figure 7(a), the loading rate dictated the stress at the start of relaxation, but not the stress reduction pattern during the relaxation phase.

The response at different temperatures is shown in Figure 7(c), with the stress relaxation behaviour alone vs. time shown in Figure 7(d). It was observed that the material behaved slightly differently at higher temperatures; the polymer was more compliant and displayed a slower stress reduction response (lower stress relaxation rate) at higher temperatures.
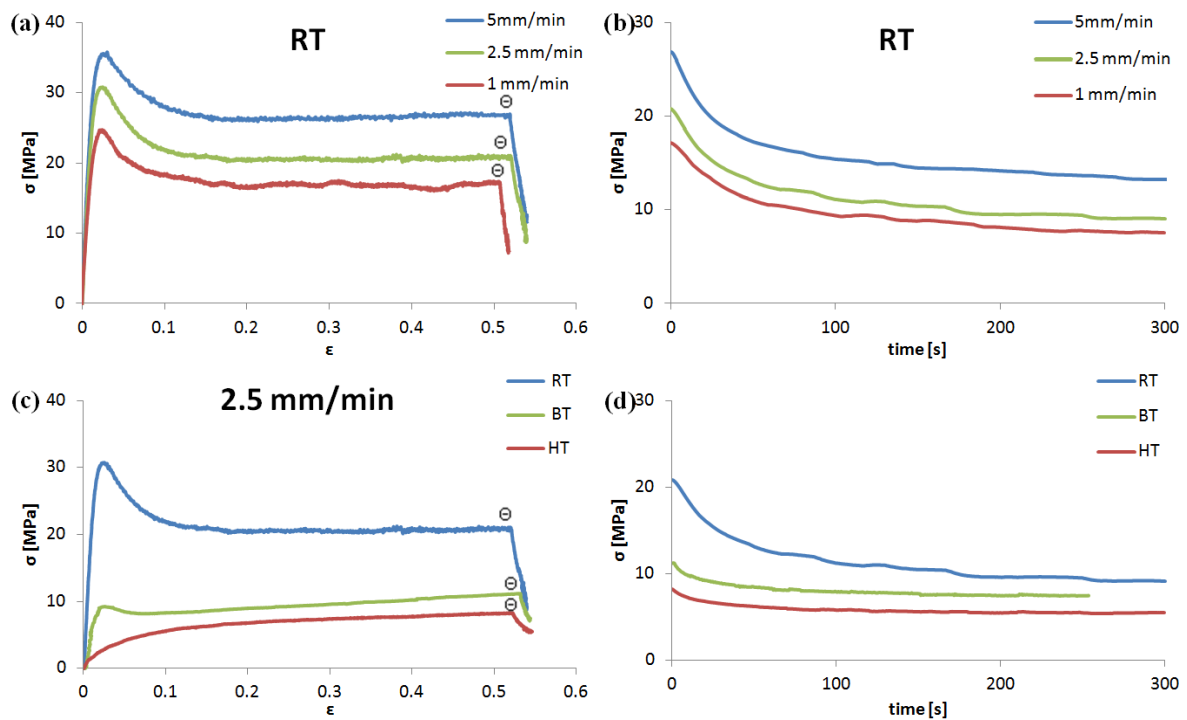

Figure 7 Relaxation-Creep test: (a) Stress-strain response at room temperature (25°C), with different loading rates up to point Θ, (b) stress vs. time for the relaxation phase at room temperature (25°C) for the different loading rate cases, (c) stress-strain response at different temperatures with a constant loading rate of 2.5 mm/min up to point Θ, and (d) stress vs. time for relaxation phase at different temperatures for a loading rate of 2.5 mm/min case.

Cyclic Loading

The results of the cyclic loading test illustrated in Figure 8 show material softening from cycle to cycle, leading to a decrease in resistance to further deformation. The top curve pattern (dotted black line in Figure 8) found in the cyclic loading test replicates the trend seen in the uni-axial tensile stress-strain behaviour. A softening process with increasing numbers of cycles was observed.
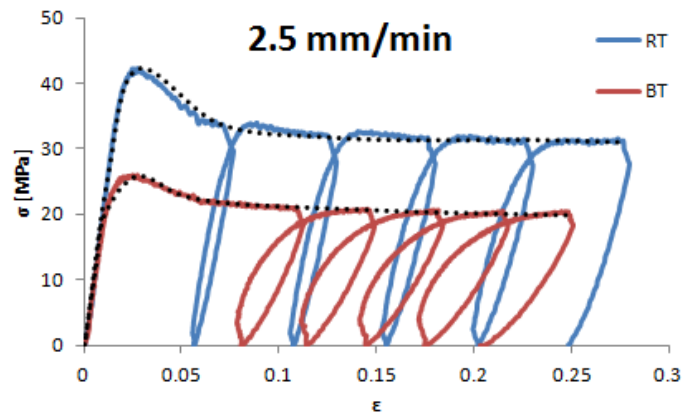
Figure 8 Experimental stress-strain response for the Cyclic test at different temperatures and a constant displacement rate of 2.5 mm/min.

4. Discussion

To fully exploit the potential of alternative non-permanent stent materials like PLLA, this paper investigates the importance of the complex mechanical behaviour (pre-degradation) showing the recovery behaviour, temperature and strain rate dependency. Previous research [32] has highlighted the dependence of Young's modulus on percentage crystallinity. For the PLLA material considered here, it is interesting to note the substantial degree of crystallinity (41.1%), determined through the DSC measurements, which undoubtedly has a bearing on the mechanical performance.

Figure 4(a) reveals the importance of strain rate dependency at room temperature, with higher stresses being generated in the material at higher strain rates, and consistent with this, a greater likelihood of specimen failure (also confirmed in previous studies [26, 28, 29]). Due to the observed fracture risk, the results indicate that the higher strain rates considered here (up to 100 mm/min equivalent displacement rate) are not advisable for practical application. The material exhibited a softer and more compliant behaviour at higher temperatures (see Figures 4(b) and 4(c)), even with a very small increase in temperature (25 - 37 - 42°C).

The behaviour on rapid unloading (Figure 4) was found to be independent of the loading strain rate. During the experiments, it was also observed that the dumbbell sample deforms more uniformly with less of a tendency towards necking and rupture at increased temperatures. This material characteristic is expected when increasing the temperature to be closer to the glass transition temperature of this polymer (60 - 65°C). PLLA is believed to behave in a brittle fashion below the glass transition temperature (T_G), and in a rubbery fashion above T_G [26]. However, in the present work, significant softening was already observed well below glass transition temperature.

Following the initial series of tests, load-unload testing was performed over a strain rate range, and up to a maximum strain, that were more directly representative of polymer stent deployment. This particular range of strain rates is associated with polymer stent deployment recommendations [28, 31]. A direct comparison of the stress-strain curves at room, body and

high temperature is shown in Figure 5(b). Apart from the smoother transition at higher temperature, as highlighted above, an increased elastic strain recovery on unloading was observed at higher temperature due to the greater elastic compliance of the material.

To focus on the recovery behaviour, the recovery test allowed the material to continue to deform in an unloaded (zero load) state for a longer time period. This test is arguably the most significant of the tests considered in this work, in the context of the balloon expandable stent deployment application, as it allows determination of the recoverable strain (instantaneous elastic and time dependent viscoelastic) and the residual permanent (plastic) strain. The recovery behaviour dictates the immediate and time dependent stent recoil on balloon deflation, and the residual permanent strain dictates the expanded stent configuration post recoil and is crucial to the prevention of stent collapse. The results (Figure 6 and Table 2) show that the material exhibited significant viscoelastic strain recovery that influenced the residual permanent strain. This effect was found to be strongly temperature dependent, with the percentage of recoverable strain increasing significantly (and consequently the percentage of permanent strain reducing significantly) over a relatively small temperature range. Understanding the relationship between elastic, viscoelastic and plastic strain behaviour, and their dependence on temperature, is of significant importance to our understanding of BP reliability in stent application. In particular, given that significant strain recovery has been observed, even at room temperature (20% = 12% elastic + 8% viscoelastic strain, Table 2), the present results indicate that PLLA in the specific form considered here would more than likely exhibit substantial recoil on balloon deflation if used in a stent application, relative to an elastic-plastic metal (stainless steel or CoCr) for example. Such substantial recovery/recoil could point to the need for stent over-expansion on deployment, so that the final stent diameter is as large as possible; however over-expansion can present risks in terms of tissue trauma.

In relation to the observed temperature dependence of the recovery, such a strong dependence might be expected if testing was performed close to the glass transition temperature of the material studied here (60 - 65°C). However, the data summarised in Table 2 reveal a strong temperature dependence of recovery even well below glass transition temperature. This result has important implications for the various specific phases in PLLA stent deployment: The polymeric material will have different mechanical behaviour at (i) room temperature (pre-implantation), (ii) during deployment at body temperature, and (iii) post-deployment at a higher temperature that could potentially be generated by an inflammatory reaction to the angioplasty procedure and the implantation of a foreign body.

The relaxation-creep tests generated further useful data on the time dependent mechanical response of the material, revealing a combination of stress relaxation and creep over time under applied crosshead displacement. The positive implication of the observed behaviour for the stent is that the reduction of stresses built up during stent deployment due to relaxation, as well as the creep behaviour, would reduce the tendency to recoil. A rather slow and stepped deployment, as suggested by the manufacturer's instructions, takes advantage of this behaviour. The effect of creep, however, may be annihilated due to the action of the compressive stress applied by the artery following balloon deflation and removal. As such, a

deployed PLLA stent could still continue to recoil, beyond the extent considered in the recovery test above (where the material was unloaded).

The cyclic loading test (see Figure 8) involved load-unload-reload deformation with increasing applied strain increments. The cyclic softening of the material is clearly evident from the results, as is the temperature dependence of the response. The results also clearly show an increased viscoelastic strain component in the overall deformation at higher temperature, as evidenced by the wider hysteresis loops in the stress-strain response (Figure 8), consistent with what was observed regarding viscoelasticity in the recovery test.

Overall, the mechanical characterisation data for PLLA presented here should be of considerable interest to design engineers for the design and development of medical devices, in particular angioplasty stents.

5. Conclusions

This paper presents a perspective into the mechanical characteristics of pre-degradation PLLA. Gaining a comprehensive understanding of the mechanical complexities of PLLA is of critical importance in to achieving the large scale realisation of PLLA as a credible stent material, and the data presented in this study is useful in this regard. The PLLA mechanical response is revealed to be highly strain rate and temperature dependent and overall strain is revealed to contain a significant recoverable (elastic and viscoelastic) component. All of these features present significant design challenges when using PLLA in the stent application. The quantified mechanical response data are valuable as input for constitutive model and finite element model development, to enable future in-silico simulation of BP stent deployment and in-vivo performance, with a view to improving the efficiency and reliability of biodegradable stenting options. The data also point to the need for the development of improved PLLA and PLLA based polymer formulations that would exhibit higher elastic stiffness and lower viscoelasticity.

16

References

[1] N. Grabow, D.P. Martin, K.P. Schmitz, K. Sternberg, Absorbable polymer stent technologies for vascular regeneration, Journal of Chemical Technology and Biotechnology, 85 (2010) 744-751.

[2] R. Waksman, Promise and challenges of bioabsorbable stents, Catheterization and Cardiovascular Interventions, 70 (2007) 407-414.

[3] N. Gonzalo, C. Macaya, Absorbable stent: focus on clinical applications and benefits, Vascular health and risk management, 8 (2012) 125.

[4] J.A. Ormiston, P.W. Serruys, E. Regar, D. Dudek, L. Thuesen, M.W. Webster, Y. Onuma, H.M. Garcia-Garcia, R. McGreevy, S. Veldhof, A bioabsorbable everolimus-eluting coronary stent system for patients with single de-novo coronary artery lesions (ABSORB): a prospective open-label trial, The Lancet, 371 (2008) 899-907.

[5] J.A. Ormiston, P.W.S. Serruys, Bioabsorbable coronary stents, Circulation: Cardiovascular Interventions, 2 (2009) 255-260.

[6] N.S. van Ditzhuijzen, A. Karanasos, J.N. van der Sijde, G. van Soest, E. Regar, Bioabsorbable Stent, in: Cardiovascular OCT Imaging, Springer, 2015, pp. 179-193.

[7] A.M. Sammel, D. Chen, N. Jepson, New Generation Coronary Stent Technology—Is the Future Biodegradable?, Heart, Lung and Circulation, 22 (2013) 495-506.

[8] R. Waksman, R. Pakala, Biodegradable and bioabsorbable stents, Current pharmaceutical design, 16 (2010) 4041-4051.

[9] R. Waksman, The Disappearing Stent: When Plastic Replaces Metal, Circulation, (2012).

[10] A.W. Chowdhury, Bioabsorbable Stents: Reaching Clinical Reality, Cardiovascular Journal, 6 (2014) 90-91.

[11] A. Bobel, S. Petisco, J.R. Sarasua, W. Wang, P. McHugh, Computational bench testing to evaluate the short-term mechanical performance of a polymeric stent, Cardiovascular Engineering and Technology, 6 (2015) 519-532.

[12] J.B. Hermiller, ABSORB III and IV: Evaluating the Safety and Effectiveness of the Absorb Bioresorbable Vascular Scaffold, Cath Lab Digest, 23 (2015).

[13] Amaranth Medical Completes MEND-II and RENASCENT Studies and Initiates Study of 120-Micron APTITUDE Sirolimus-Eluting Bioresorbable Scaffold, in, http://amaranthmedical.com/, 2015.

[14] A. Abizaid, R.A. Costa, J. Schofer, J. Ormiston, M. Maeng, B. Witzenbichler, R.V. Botelho, J.R. Costa, D. Chamié, A.S. Abizaid, Serial multimodality imaging and 2-year clinical outcomes of the novel DESolve novolimus-eluting bioresorbable coronary scaffold system for the treatment of single de novo coronary lesions, JACC: Cardiovascular Interventions, 9 (2016) 565-574.

[15] REVA Releases Positive Initial Results for Fantom at TCT 2015 in, http://www.teamreva.com/, 2015.

[16] R.L. Varcoe, O. Schouten, S.D. Thomas, A.F. Lennox, Initial Experience With the Absorb Bioresorbable Vascular Scaffold Below the Knee Six-Month Clinical and Imaging Outcomes, Journal of Endovascular Therapy, 22 (2015) 226-232.

[17] N. Weir, F. Buchanan, J. Orr, G. Dickson, Degradation of poly-L-lactide. Part 1: in vitro and in vivo physiological temperature degradation, Proceedings of the Institution of Mechanical Engineers, Part H: Journal of Engineering in Medicine, 218 (2004) 307-319.

[18] L.S. Nair, C.T. Laurencin, Biodegradable polymers as biomaterials, Progress in Polymer Science, 32 (2007) 762-798.

[19] J.C. Middleton, A.J. Tipton, Synthetic biodegradable polymers as orthopedic devices, Biomaterials, 21 (2000) 2335-2346.

[20] K.A. Athanasiou, C.M. Agrawal, F.A. Barber, S.S. Burkhart, Orthopaedic applications for PLA-PGA biodegradable polymers, Arthroscopy: The Journal of Arthroscopic & Related Surgery, 14 (1998) 726-737.

[21] C.M. Agrawal, G.G. Niederauer, K.A. Athanasiou, Fabrication and characterization of PLA-PGA orthopedic implants, Tissue engineering, 1 (1995) 241-252.

[22] H. Chuah, D. Lin-Vien, U. Soni, Poly (trimethylene terephthalate) molecular weight and Mark–Houwink equation, Polymer, 42 (2001) 7137-7139.

[23] N. Grabow, C.M. Bünger, K. Sternberg, S. Mews, K. Schmohl, K.P. Schmitz, Mechanical properties of a biodegradable balloon-expandable stent from poly (l-lactide) for peripheral vascular applications, Journal of Medical Devices, 1 (2007) 84.

[24] N. Grabow, M. Schlun, K. Sternberg, N. Hakansson, S. Kramer, K.P. Schmitz, Mechanical properties of laser cut poly (L-lactide) micro-specimens: implications for stent design, manufacture, and sterilization, Journal of biomechanical engineering, 127 (2005) 25.

[25] S.K. Eswaran, J.A. Kelley, J.S. Bergstrom, V.L. Giddings, Material Modeling of Polylactide.

[26] Y. Wong, Z. Stachurski, S. Venkatraman, Modeling shape memory effect in uncrosslinked amorphous biodegradable polymer, Polymer, 52 (2011) 874-880.

[27] N. Weir, F. Buchanan, J. Orr, D. Farrar, G. Dickson, Degradation of poly-L-lactide. Part 2: increased temperature accelerated degradation, Proceedings of the Institution of Mechanical Engineers, Part H: Journal of Engineering in Medicine, 218 (2004) 321-330.

[28] N. Debusschere, P. Segers, P. Dubruel, B. Verhegghe, M. De Beule, A finite element strategy to investigate the free expansion behaviour of a biodegradable polymeric stent, J Biomech, 48 (2015) 2012-2018.

[29] S. Petisco Ferrero, Biodegradable thermoplastic elastomers: tuning viscoelastic properties and shape memory, (2015).

[30] H. Tsuji, Y. Ikada, Properties and morphology of poly (L-lactide). II. Hydrolysis in alkaline solution, Journal of Polymer Science Part A: Polymer Chemistry, 36 (1998) 59-66.

[31] Abbott, Absorb GT1 Bioresorbable Vascular Scaffold System, IFU, http://eifu.abbottvascular.com/, 2015.

[32] J.R. Sarasua, Crystallinity and mechanical properties of optically pure polylactides and their blends, Polymer Engineering and Science, 45(2005) 745-753.

List of Figure Captions

Figure 1 Specimen preparation: A - PLLA granules, B - PLLA-DCM solution, C - Glass dish with PLLA solution, D - PLLA film specimen and rubber grip preparation, E - PLLA specimen in tensile testing machine.

Figure 2 Terminology to describe typical stress-strain behaviour of a PLLA polymer upon loading and unloading.

Figure 3 DSC thermogram.

Figure 4 Experimental stress-strain behaviour at different displacement rates: (a) At room temperature (25°C), (b) at body temperature (37°C), and (c) at high temperature (42°C).

Figure 5 Experimental stress-strain behaviour with max displacement of 50%: (a) At room temperature (25°C) and different displacement rates, (b) at different temperatures and a displacement rate of 2.5 mm/min, and (c) distribution of data over a number of specimens tested at room temperature and a displacement rate of 2.5 mm/min.

Figure 6 Recovery test: (a) Experimental stress-strain response for the recovery test at different temperatures and maximum gauge strains, with a constant loading displacement rate of 2.5 mm/min, and (b) recoverable strain (as a percentage of total strain) as a function of temperature, over a temperature range of 25 to 42°C.

Figure 7 Relaxation-Creep test: (a) Stress-strain response at room temperature (25°C), with different loading rates up to point Θ, (b) stress vs. time for the relaxation phase at room temperature (25°C) for the different loading rate cases, (c) stress-strain response at different temperatures with a constant loading rate of 2.5 mm/min up to point Θ, and (d) stress vs. time for relaxation phase at different temperatures for a loading rate of 2.5 mm/min case.

Figure 8 Experimental stress-strain response for the Cyclic test at different temperatures and a constant displacement rate of 2.5 mm/min.